JOURNAL OF THERMOPHYSICS AND HEAT TRANSFER
Vol. 6, No. 3, July–Sept. 1992

Arc Transition and Growth of Big-Arcs in Magnetohydrodynamics Generator Channels

K. A. Satheesh,* Y. Okumura,† and K. Okazaki‡
Toyohashi University of Technology, Toyohashi, 441, Japan

The arc transition in MHD generator channels from a low-current micro-arc mode to a high-current big-arc mode has been studied. An arc model, which considers the arc region to include an arc spot, an arc column, and a current spreading zone, has been proposed to obtain the critical parameters for such a transition. The model specifically aims at studying the possibilities for the occurrence of arcs that may extend up to, or beyond the thermal boundary layers, which has been reported in some experimental observations. The model predicts the critical values for the growth of such arcs, and were found to compare well with experimental observations.

Nomenclature

A_a = $1.53 \times 10^{-2}/\Lambda$
A_R = Richardson's constant, taken to be 1.20×10^6A/(m^{2}K^2)
$\bar{b}_0$ = $Ze^2/(12\pi\varepsilon_0 kT)$
C, C_p = specific heat at constant pressure, J/(kg·K)
C_{ft} = function of $\alpha\tau/r^2$
d = characteristic length for cooling of the electrode, 0.01 m, for the given experimental conditions
E_a = arc column electric field, V/m
e = electronic charge, C
f = constant in Eq. (6), 0.26
h = heights of various arc regions, m
I_a = arc current, A
J = current density, A/m^2
k = Boltzman constant, $1.38*10^{-23}$ J/K
ℓ, L = characteristic lengths for heat loss in the transverse (normal to electrode surface) and the radial directions, respectively, m
l_D = $(\varepsilon_0 kT/n_e e^2)^{1/2}$ is the Debye's length
m, n = exponents in the relationship for Nusselt number with Reynold's and Prandtl numbers
n_e = number density of electrons, m^{-3}
n_i = number density of ions, m^{-3}
Pr = Prandtl number
Q = heat loss term, W
Re = Reynold's number
r = radii of various arc regions, m
S_1 = steady-state temperature gradient, K/m
T = temperature, K
T_s = arc spot temperature, K
u = gas velocity, m/s
V = voltage drops V
$\bar{V}_i$ = average thermal velocity of ions, m/s
x = distance from leading edge, m
Y_{spr} = total arc length from electrode surface to top of current spreading region
y = transverse distance from electrode surface, m
Z = charge on the nuclei
α = thermal diffusivity, m^2/s
β = ratio of gas velocity at any distance y and the main stream velocity
γ = exponent in the temperature dependence of electrical conductivity
δ = boundary-layer thickness, m
ε_0 = $8.854*10^{-12}$ F/m, is the permittivity of free space
θ = the parameter in the solution of the heat-conduction equation (Eq. 4) in units of rad/m
Λ = $l_D/\bar{b}_0$, may be interpreted as the impact parameter for a 90-deg scattering
λ = thermal conductivity, W/(m·K)
μ = dynamic viscosity, Pa·s
ν = kinematic viscosity, m^2/s
ξ = ratio of the gas velocity in the arc region to the ambient gas velocity, 0.8
ρ = gas mass density, kg/m^3
σ = plasma electrical conductivity, S/m
τ = characteristic times, s
Φ_e = $\phi_e + 2kT_s/e$
Φ_{el} = $\phi_e + 2kT_{el}/e$
Φ_i = $\phi_i - \phi_e$
ϕ_e = effective electron work function of cathode surface, eV
ϕ_i = ionization potential of neutral seed atoms, eV

Subscripts

a = arc column parameters
∞ = main flow parameters
d = diffuse region values
e = electronic component of the parameter
el = electrode
g = gas or plasma outside the arc
i = ionic component of the parameter
l = value at a distance ℓ in the electrode, from the surface
m = metallic or electrode value
o = reference values
r = radial component
s = arc spot parameter
spr = current spreading region parameter
T = temperature
w = electrode wall
x, y = x and y direction components

Introduction

IN MHD generator channels, the current transport in the near-electrode cold boundary layers, inevitably tends to be in the arc mode at operational current densities. The transition from a uniform current transport at very low current densities to a constricted or arcing discharge at higher current densities has been very widely studied,[1-7] and is a well understood phenomenon. However, as mentioned, arcing in MHD channels is almost unavoidable and, hence, a detailed study

Received April 22, 1991; revision received July 9, 1991; accepted for publication July 11, 1991.

*Associate Researcher, Department of Energy Engineering.
†Graduate Student, Department of Energy Engineering.
‡Associate Professor, Department of Energy Engineering.

of the arc regime itself becomes very important in minimizing the damage caused by the arcs.

The arcs that occur in MHD generator channels have been broadly classified into two types[8-14]; namely, the micro-arcs and the big arcs. The micro-arcs carry very low currents (~1 A) and have very short lifetimes (~μs), but they are highly mobile, moving rapidly down the flow and along the electrode surface with large velocities (~m/s).[13,15] The big arcs carry much larger currents (100 A or more), have longer lifetimes (~ms),[14] and are much less mobile.[13] The intense heating in the arc spots in the big-arc mode is the main cause for electrode damage in MHD channels. Hence, it is clear that the best choice in order to achieve long-duration operation of the electrodes will be to find an effective method to suppress the big-arc stages. This requires a clear understanding of the controlling mechanisms for the transition from the micro-arc regime to the big-arc regime.

The existence of two arc regimes at the cathode has been clarified experimentally and theoretically.[14-17] Okazaki et al.[14] obtained two clearly separated arc regimes, with micro-arcs having currents of about 1 A and big arcs carrying currents of about 100 A. The transition from micro-arc to big arc occurred when the cathode drop increased to 270 V. Buznikov et al.[15] developed a theoretical model for arcs, which differed from the previous models (see Rosa[18]) in that it included, in the spreading region, a region of nonequilibrium conductivity defined by two reference electric fields, in addition to an equilibrium hemispherical spreading part. They obtained two minima in the boundary layer voltage drop, corresponding to arc heights of the order of a laminar sublayer thickness, at low current densities, and at about 0.3 δ (where δ is the boundary-layer thickness), at higher current densities. Furthermore, from an experimental study in a supersonic channel, Buznikov et al.[16] obtained a critical current density for the transition from micro-arc to big arc, which increased with increasing Mach number. However, the cause, or the controlling mechanism for such a transition was not clarified. In Ref. 17, it has been suggested that surface effects, especially the effective work function of the seed-deposited cathode surface, plays an important role in the transition from the micro-arc to the big-arc mode. An increase in the work function value was found to produce a large increase in the values of arc current and arc spot temperature.[17]

Generally, it is considered that the arcs in an MHD generator channel are confined to the near-electrode boundary layers and that the current transport in the main flow is always diffuse. However, the results from a recent experimental study[19] reveal that the arcs extended not only beyond the thermal boundary layer, but also even up to the anode, effectively short-circuiting the plasma. The reason for such an extreme behavior should be the low plasma electrical conductivity caused by very low seeding rates, in these experiments. Although such an extreme arc behavior is not common in MHD channels, the extension of arcs beyond the boundary layers into the flowing plasma, producing tail-like structures, is a widely observed phenomenon. The arcs in the big-arc mode generally have larger dimensions, and may extend beyond the thermal boundary layer and get dragged by the flow. Because these are the arcs that carry very high currents and, hence, the most damaging as far as MHD channels are concerned, it is very important to understand the circumstances for the occurrence and the extension beyond the boundary layer of such high-current arcs.

Most of the theoretical arc models[15,18] consider a minimum voltage principle, which assumes that the arc adjusts its height so as to minimize the overall boundary-layer voltage drop. Because the arc is no longer considered as necessarily confined to the boundary layer, this minimum principle does not hold true for such arcs. Furthermore, most of these arc models do not consider the arc spot region. In Ref. 15, the arc spot voltage drop was considered as a very weak function of arc current, effectively contributing to an almost constant, small voltage drop. However, as has been suggested in Ref. 17, the effective work function of the composite electrode surface may have a significant role in the arc transition process, hence, the spot region has to be included in the arc model.

In the present analysis, an arc model has been proposed that considers the arc region to be made up of an arc spot, an arc column, and a current spreading region. It is assumed that the arc current (which itself may be governed by parameters external to the arc, such as core plasma current density) determines the values of the arc region parameters. The minimum voltage drop principle has been modified so that the arc height no longer restricts the arc to the boundary layer. The present model not only obtains the optimum arc parameters but also predicts the critical values for the growth of big arcs, which may extend up to, or beyond, the boundary layer.

Analysis

The arc model considers an arc spot, an arc column, and a current spreading region. A schematic representation of the arc model considered is shown in Fig. 1. If the arc extends beyond the boundary layer, a diffuse current transport region within the boundary layer will not exist. Hence, for arcs that have heights (arc column plus spreading region heights) equal to or greater than the thermal boundary-layer thickness, the overall voltage drop will not have a diffuse region component. The arc is assumed to support an arc current for which the arc region voltage drop will be a minimum. The arc column height is chosen such that the minimum in the voltage drop occurs when the total arc height equals the thermal boundary-layer thickness, or when the diffuse region voltage drop vanishes. In order to find this arc height, a diffuse current transport region is also considered initially (shown by the dotted lines in Fig. 1), which, however, vanishes when the critical arc height is reached.

Arc Spot

The arc spot is the region that connects the arc column to the conducting electrode. This region, being located at the coldest part in the channel, can have large voltage drops, which should depend strongly on the surface effects at the cathode.

The model for an arc spot burning at the cathode surface considers an energy-balance equation in which, the heat liberated within the spot due to ion bombardment is balanced by the energy carried away by the thermionically emitted electrons, and the loss due to the thermal conduction cooling, given by

$$\pi r_s^2[J_i(V_s + \Phi_i) - J_e\Phi_e] + Q = 0 \qquad (1)$$

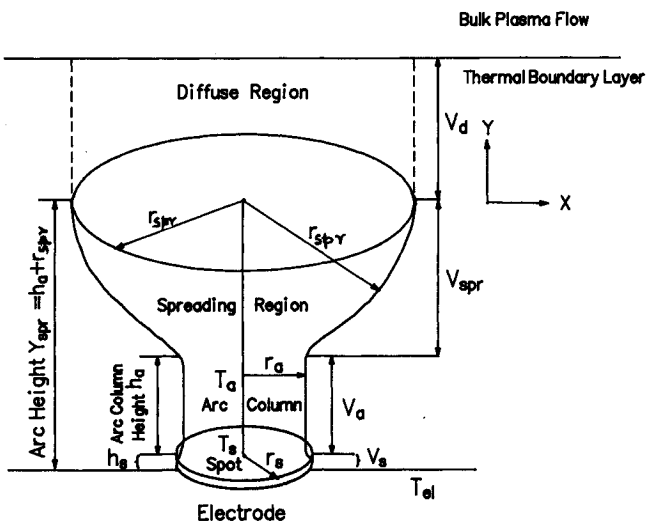

Fig. 1 Schematic representation for the arc model.

where $J_i(V_s + \Phi_i) = J_i[V_s + (\phi_i - \phi_e)]$ and $J_e\Phi_e = J_e(\phi_e + 2kT_s/e)$ are the energy transported by the ion flux and the energy carried away by the emitted electrons, respectively.[20]

The overall heat loss term Q can be expressed as the sum of the radial and the transverse heat loss terms, as

$$Q = Q_r + Q_y \tag{2}$$

where

$$Q_r = 2\pi r_s h_s \lambda_g \left[\frac{1}{r}\frac{dT}{dr} + \frac{d^2T}{dr^2}\right] L \text{ and } Q_y = \pi r_s^2 \lambda_m \frac{d^2T}{dy^2} l$$

Q_r is the radial component of the heat conduction term and Q_y is the heat conducted away by the electrode; h_s is a parameter equivalent to the spot height or spot thickness.

Assuming an exponential temperature decrease, the heat conduction loss in the radial direction is obtained as

$$Q_r = 2\pi r_s h_s \lambda_g (T_s - T_{el}) \left(\frac{1}{L} - \frac{1}{r_s}\right) \tag{3}$$

where T_{el} is the electrode temperature far from the spot, and λ_g, the gas thermal conductivity, is assumed to be independent of r.

For heat conduction by the electrode, a one-dimensional nonsteady heat conduction law, for a slab of thickness l = in the y-direction, but infinite in other directions, was assumed, as

$$\frac{\partial T}{\partial t} = \alpha_m \frac{\partial^2 T}{\partial y^2}$$

where $\alpha_m (= \lambda_m/(\rho_m C_m))$ is the thermal diffusivity of the electrode material. This equation has a solution of the form[21]

$$T = [A \cos(\theta y) + B \sin(\theta y)]\exp(-\theta^2 \alpha_m \tau)$$

where the quantities A, B, and θ may be obtained using the boundary and initial conditions

$$y = 0, \quad T = T_s, \quad \text{at } t = \tau_a; \qquad y = 0, \quad \frac{\partial T}{\partial y} = S_1$$

$$\text{at } t = 0; \qquad y = l, \quad T = T_l, \quad \text{at } t = 0$$

Here, τ_a is the arc lifetime and S_1 is the steady-state temperature gradient.

The heat conduction in the axial direction was then obtained as

$$Q_y = C_4 \pi r_s^2 \tag{4}$$

where $C_4 = -\lambda_m l \theta^2 T_s$, and θ is given by the equation

$$T_l - T_s e^{\theta^2 \alpha_m \tau_a} \cos(\theta l) + [(T_s - T_l)/\theta l] \sin(\theta l) = 0$$

The importance of Eq. (4) lies in the fact that the heat conducted away through the electrode makes the most significant contribution to heat removal from the excess heat liberated within the arc spot.

The spot radius r_s is given by $r_s^2 = I_a/(\pi J_s)$, where I_a is the arc current, $J_s (= J_i + J_e)$ is the total arc spot current density, and J_i is the ion current density, given by

$$J_i = \tfrac{1}{4} n_i e \bar{V}_i$$

where, the number density of ions n_i has been assumed to be that given by the Saha equation at the arc temperature T_a. The thermionic emission current density J_e is given by the Richardson-Dushman equation

$$J_e = A_R T_s^2 \exp\left(-\frac{e\phi_e}{kT_s}\right)$$

where, the Schottky effect has not been considered because the electric field strength in the arc regime is not large enough to affect the work function. Equation (1) can then be solved to obtain the arc spot voltage drop as a function of the arc current, provided the arc spot temperature T_s and the arc temperature T_a are known. The arc spot temperature T_s has been related to arc spot voltage drop and arc spot current,[22] and the variation of spot temperature with arc temperature has been obtained in an earlier study.[17] Hence, the arc spot voltage drop V_s can be obtained as a function of only the arc current I_a, for given values of arc temperature T_a and work function ϕ_e of the electrode surface, from the expression[17]

$$V_s = D_1/(A_1 + B_1) \tag{5}$$

where

$$A_1 = 2h_S\lambda_g(C_{ft}/\lambda_{el})[1/L - (\pi J_s/I_a)^{1/2}]\,\pi J_s$$

$$B_1 = J_i - (2k/e)[(d\langle J\rangle/\lambda_{el}) + (C_{ft}/\lambda_{el})(\pi J_s I_a)^{1/2}]J_e$$

$$D_1 = J_e\Phi_{el} - J_i\Phi_i - C_4; \quad \Phi_{el} = \phi_e + 2kT_{el}/e$$

Here, C_{ft} is a function of $(\alpha\tau/r_s^2)$, which depends upon the heat flux to the electrode through the arc spot area,[17,22] and $\langle J\rangle$ is the average current density through the electrode.

Arc Column

The arc column has been considered as a solid cylinder of radius r_a and height h_a. The plasma temperature in this cylindrical region has been assumed to be constant at T_a, which has been defined as the arc temperature. The arc temperatures being extremely high, the electrical conductivity in the arc column has been assumed to be that given by a three-halves power law.

The energy-balance equation for such a system can be expressed in the form[18,23]

$$I_a E_a = f\pi Pr^m \lambda_a (\Delta T) Re^n \tag{6}$$

where

$$Pr = (\nu_a/\alpha_a) = (\mu_a C_{pa}/\lambda_a)$$

is the Prandtl number

$$Re = (\rho_a u_a D_a/\mu_a) = (2\rho_a u_a r_a/\mu_a)$$

is the Reynold's number; and $\Delta T = T_a - T$ = arc temperature − ambient temperature. Also, $u_a = \xi u_g$ where u_g, the ambient gas velocity, is assumed to be given by that for a laminar flow

$$(u_g/u_\infty) = 1 - [(1 - (y/\delta))]^4 = \beta \tag{7a}$$

where u_∞ is the mainstream plasma velocity and δ is the velocity boundary-layer thickness. Because the Prandtl number for a combustion plasma is close to unity, the thermal and velocity boundary-layer thicknesses may be assumed to be equal; then, the thermal boundary-layer thickness δ_T for a laminar flow (taking the Blasius solution for the boundary layer on a flat plate) can be written as[21]

$$(\delta_T/x) \approx (5.0/\sqrt{Re_x})$$

where

$$Re_x = (ux/\nu) = (\rho ux/\mu)$$

is the Reynold's number, x is the distance from the leading edge (a value of $x = 0.0685$ m has been obtained from experimental determinations[19]). The kinematic viscosity ν was calculated for a temperature that was the average of electrode and plasma temperatures.

Then, the ambient temperature profile can also be written in the form

$$(T - T_{el})/(T_\infty - T_{el}) = \beta \tag{7b}$$

hence

$$\Delta T = T_a - T = T_1 - T_2\beta \tag{7c}$$

where

$$T_1 = T_a - T_{el} \quad \text{and} \quad T_2 = T_\infty - T_{el}$$

The arc column radius can be given as

$$r_a = \left(\frac{I_a}{\pi J_a}\right)^{1/2} = \left(\frac{I_a}{\pi \sigma_a E_a}\right)^{1/2}$$

where σ_a is the plasma electrical conductivity in the arc column. Because the gas temperature itself is very high in the arc column, there may not be a significant elevation of the electron temperature over that of the gas temperature. The electrons are also in a perpetual state of exchange of their energies with the heavy species. Hence, both the electron and gas temperatures in the arc column are assumed to be the same and equal to T_a, the arc temperature. The electrical conductivity in the arc column is then assumed to be that given by a three-halves power law, as[24]

$$\sigma_a = A_a T_a^{3/2}$$

where, $A_a = 1.53 \times 10^{-2}/(\ell n \Lambda)$, and the value of $(\ell n \Lambda)$ has been obtained from Mitchner and Kruger,[24] corresponding to the arc temperature T_a.

Substituting the above relations into Eq. (6), the electric field in the arc column can be obtained as

$$E_a = A^{2/(n+2)}\,(T_1\beta^n - T_2\beta^{n+1})^{2/(n+2)}\, I_a^{(n-2)/(n+2)} \tag{8}$$

where

$$A = f\pi\mu_a^{m-n}\lambda_a^{1-m}C_{pa}^m(2\rho_a u_\infty \xi)^n/(\pi\sigma_a)^{n/2}$$

Then, the voltage drop in the arc column can be obtained by integrating Eq. (8) over the arc column height, as

$$V_a = \int_{h_s}^{h_a} E_a \, dy$$

which yields the following expression:

$$V_a = A_4 I_a^{n_2}\left[\beta^{n_3}(T_1 - T_2\beta)^{n_4}\Big/\left\{\left(1 - \frac{y}{\delta_T}\right)^3 \cdot [nT_1 - (n+1)T_2\beta]\right\}\right]_{h_s}^{h_a} \tag{9}$$

where

$$n_2 = \frac{n-2}{n+2}, \quad n_3 = \frac{3n+2}{n-2}, \quad n_4 = \frac{n+4}{n+2}$$

$$\text{and} \quad A_4 = \frac{A^{2/(n+2)}}{(4/\delta_T)n_3}$$

Also, substituting for E_a from Eq. (8), the arc column radius can be obtained as

$$r_a = A_5[(T_1 - T_2\beta)\beta^n]^{-1/(n+2)} I_a^{(1-n_2)/2} \tag{10}$$

Current Spreading Region

The most commonly chosen model for the current spreading region is that of a hemispherical current spread. In the actual situation, arcs, especially the big arcs, are generally seen to be dragged along the flow direction, producing tail-like structures. However, the micro-arcs, being small and confined to the boundary layer, could be assumed to possess a definite structure. Because the drag force is stronger outside the boundary layer, the big arcs also may be assumed to have a somewhat definite shape initially, before they grow to large sizes extending outside the boundary layer. Hence, a hemispherical current spreading region has been assumed in the present analysis, for the sake of simplicity. The voltage drop for such a spreading zone can be written as

$$V_{spr} = \frac{I_a}{2\pi}\int_{r_a}^{r_{spr}} \frac{dr}{\sigma_{spr} r^2} \tag{11}$$

where r_a is the radius at the top of the arc column, and r_{spr} is the radius at which $I_a/(\pi r_{spr}^2) = J_\infty$, the main plasma current density. The conductivity in the spreading region is a function of the radial distance from the column r and, hence, for each value of radius r, there corresponds a conductivity such that $r = u\tau$ (if we assume the constant of proportionality to be unity); here u is the ambient gas velocity at a distance y from the wall, and τ is the recombination time for that conductivity. For such a case, the electrical conductivity may be written as[18]

$$\sigma_{spr} \approx \sigma_0 \tau_0^{n_1} u^{n_1}/r^{n_1} \tag{12}$$

where σ_0 and τ_0 are some reference values of σ and τ. For electron three-body recombination, values of $\sigma_0 = 120$ S/m, $\tau_0 = 10^{-7}$ s and $n_1 = \frac{1}{3}$ could be chosen.[18]

Substituting for the gas velocity $u = u_g$ (the ambient gas velocity) from Eq. (7a), the voltage drop in the spreading region can be written as

$$V_{spr} = \frac{I_a}{2\pi\sigma_0(u_\infty\tau_0)^{n_1}}\int_{r_a}^{r_{spr}} \frac{dr}{\beta^{n_1} r^{2-n_1}}$$

Substituting for r_a from Eq. (10) and for $r_{spr} = (I_a/\pi J_\infty)^{1/2}$, the spreading region voltage drop can be obtained as

$$V_{spr} = A_6\beta_c^{-n_1} I_a^{(1+n_1)/2} - A_7\beta_a^{n_5}(T_1 - T_2\beta_a)^{n_6} I_a^{n_7} \tag{13}$$

where $\beta_c = 1 - (1 - Y_{spr}/\delta_T)^4$; $Y_{spr} = h_a + r_{spr}$, is the distance from the electrode surface to the top of the spreading region (because h_s is many orders lower than h_a, it will not make any contribution to this overall arc height). Hence

$$\beta_c = 1 - \left\{1 - \left[h_a + \left(\frac{I_a}{\pi J_\infty}\right)^{1/2}\right]\frac{1}{\delta_T}\right\}^4$$

$$\beta_a = 1 - \left[1 - \frac{h_a}{\delta_T}\right]^4; \quad A_6 = B_6(\pi J_\infty)^{(1-n_1)/2}$$

$$B_6 = \frac{1}{2\pi\sigma_0(u_\infty\tau_0)^{n_1}(n_1 - 1)}$$

$$A_7 = B_6 A^{n_6}(\pi\sigma_a)^{(1-n_1)/2}; \quad n_5 = [n - 2n_1(n+1)]$$

$$n_6 = (1 - n_1)/(n+2); \quad n_7 = (n + 2n_1)/(n+2)$$

Diffuse Region

The diffuse region voltage drop may be expressed by a simple relation

$$V_d = J_\infty \int_{Y_{spr}}^{\delta_T} \frac{dy}{\sigma}$$

where

$$Y_{spr} = h_a + r_{spr} \tag{14}$$

The electrical conductivity σ is assumed to be given by a power law

$$\sigma = \sigma_\infty [-(T/T_\infty)]^\gamma$$

where the value of the component γ is generally found to vary from 10 to 12, for combustion products plasma. The lower value of $\gamma = 10$ has been chosen in the present calculations, to fit the experimental conditions.

A linear temperature profile has been assumed for the diffuse region, with the temperature at the top of the spreading region (i.e., $y = Y_{spr}$) considered as that given by the ambient temperature profile

$$T = T_{el} + (T_\infty - T_{el})y/\delta_T$$

Then

$$\sigma = \sigma_\infty (a + by)^\gamma$$

where

$$a = \frac{T_{el}}{T_\infty} \quad \text{and} \quad b = (1 - a)/\delta_T$$

Hence, the voltage drop in the diffuse current transport region can be obtained as

$$V_d = \frac{J_\infty}{\sigma_\infty} \int_{Y_{spr}}^{\delta_T} \frac{dy}{(a + by)^\gamma} = \frac{J_\infty}{(1 - \gamma)\sigma_\infty} [(a + b\delta_T)^{(1-\gamma)} - (a + bY_{spr})^{(1-\gamma)}] \tag{15}$$

Now, the total boundary-layer voltage drop can be obtained as the sum of the arc spot voltage drop (Eq. (5)), the arc column voltage drop, (Eq. (9)), the spreading region voltage drop (Eq. (13)), and the diffuse region voltage drop (Eq. (15)):

$$V_b = V_s + V_a + V_{spr} + V_d \tag{16}$$

Then, by assuming that the arc will adjust the arc current so as to minimize the overall voltage drop, the optimum arc parameters could be obtained. However, this requires knowledge of the values of arc temperature and effective work function of the seed-deposited cathode surface. Because there were no matching data available for arc temperature, the calculations were carried out for different values of arc temperature. In the case of effective work function of the composite electrode surface, it is expected that in the high-current arc mode, the work function should increase to very high values.[17,25] This occurs because, in the transition from micro-arc to the high-current big-arc mode, the deposited seed layer gets removed to a large extent, or almost entirely; thereby, effectively increasing the work function values closer to that of the clean metallic surface.[17] Furthermore, in the big-arc mode, the work function value was found to remain almost constant.[25] Hence, choosing a constant work function value, at least in the big-arc mode, may be well justified. However, in the present calculations, the work function value was varied in order to estimate its impact on the arc parameters.

Results and Discussion

The calculations have been performed for a kerosine combustion products plasma with very low potassium seeding (0.0415 wt%). The values of the thermophysical properties (α, λ, ν, and C_p) for the chemical combustion products (CO_2, H_2O and N_2) and that for the properties of the electrode material (stainless steel, SS-304) have been taken from standard tables. The calculated results have been compared with the experimentally obtained data in Ref. 19, wherever possible.

Figures 2 and 3 show the effect of work function ϕ_e of the composite cathode surface on arc region voltage drops. From Fig. 2 it can be seen that an increase in work function causes a large increase in the cathode voltage drop. This increase in cathode drop was identical for all the electrode temperatures considered, with a higher electrode temperature producing a slightly lower voltage drop. (The dependence of ϕ_e on the electrode temperature was not considered because it was not known. This resulted in much larger emission current densities, hence, lower voltage drops at the higher electrode temperatures.) The increase of cathode drop with an increase in work function can be understood more clearly from Fig. 3. As expected, it is mainly the arc spot voltage drop that increases with increasing work function value. The arc column voltage drop is unaffected by the change in ϕ_e. The spreading region voltage drop shows a small increase, which may be due to slight changes in the arc parameters caused by the change in ϕ_e. The overall voltage drop, hence, increases, mainly as a reflection of the increase in the spot region voltage drop. An increase in the value of the effective work function, which will accompany a change in the arcing conditions, is an indicator of an increasing arc activity. Therefore, for higher values of ϕ_e, the arc should be more intense; hence, more damaging. This result is in good agreement with earlier observations.[17,25] However, these results will be more convincing if the arc temperature were also a related function, instead of the constant value that has been taken in the present calculations. Nevertheless, the behavior of the voltage drops with increasing effective work function is quite expected.

Figure 4 shows the variation of overall cathode voltage drop with increasing plasma current density, for different values of arc temperature. The cathode voltage drop initially shows a

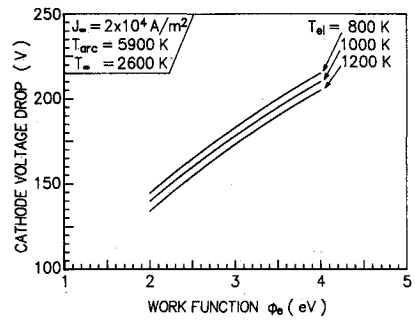

Fig. 2 Variation of cathode voltage drop with the effective work function, for different electrode temperatures.

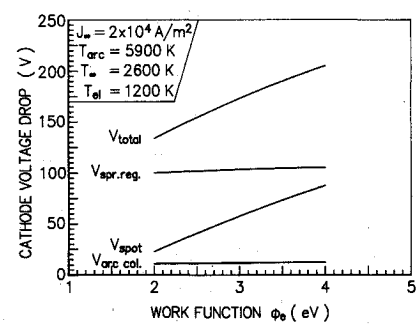

Fig. 3 Dependence of arc region voltage drops on the effective cathode work function.

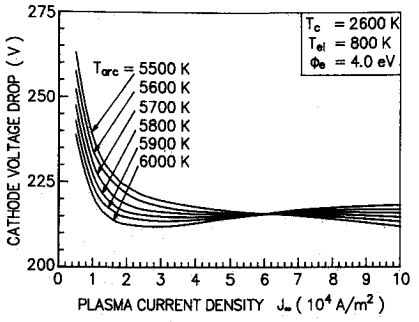

Fig. 4 Variation of cathode voltage drop with main plasma current density, for different arc temperatures.

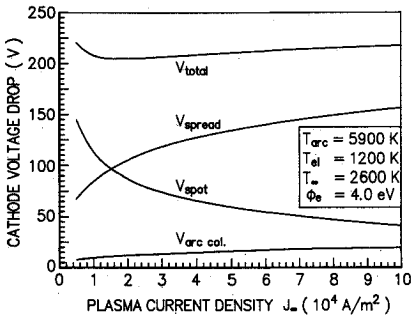

Fig. 5 Variation of the various arc region voltage drops with main plasma current density.

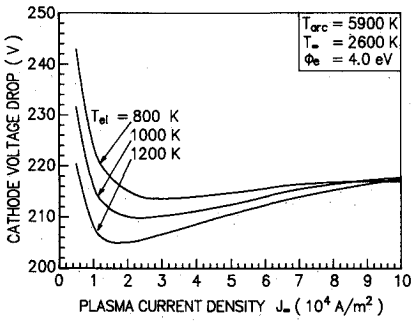

Fig. 6 Dependence of cathode voltage drop on main plasma current density for different electrode temperatures.

large decrease with increasing plasma current density for all arc temperature values. However, for the higher values of arc temperature, the cathode drop shows a minimum and then, increases slowly with increasing plasma current density. This behavior of the overall voltage drop may indicate the occurrence of a transition in the arc discharge, which in this case should correspond to the transition to the big-arc mode. Therefore, this minimum value of the cathode drop and the corresponding value of the plasma current density could be considered as the critical values for the transition from the micro-arc to the big-arc mode. The minimum in the voltage drop appears for arc temperatures above 5800 K, and the behavior is quite clear at an arc temperature of 5900 K. Hence, this arc temperature has been used in all the other calculations.

The initial decrease in the overall voltage drop is due to the drastic decrease in the value of arc spot voltage drop with an increase in the plasma current density, at lower values of the current density. This is seen more clearly in Fig. 5. The very high values of spot region voltage drop suggest that the spot region is very resistive at low current densities and will make a significant contribution to the arc region voltage drop in the low-current micro-arc mode and in the transition stages of the big-arc mode, but becomes less significant in the high-current big-arc mode. This should be due to the attainment of a constant effective work function value (of about 3eV–4eV) by the cathode surface in the big-arc mode.[17,25] Furthermore, in the micro-arc mode, the distinction between the spot and the arc column may not be very sharp.

The effect of electrode temperature on the variation of cathode voltage drop with plasma current density is shown in Fig. 6. It can be seen that the critical values of the current density as well as the cathode drop decreases slightly with increasing electrode temperature. These critical values can be compared with the experimentally obtained critical values from Ref. 19. The theoretical and experimental voltage drops show good agreement, as can be seen in Fig. 7. However, the values of the critical current density obtained from the theoretical analysis are much higher than that obtained experimentally in Ref. 19 (where the mean value of critical current density for the occurrence of big-arcs have been obtained). This difference may be explained as follows. In the theoretical arc model, the spreading region radius r_{spr} was defined as the radius at which $I_a/\pi r_{spr}^2 = J_\infty$, the diffuse or main plasma current density. This, then, considers the main plasma current density to be the current density just above the spreading region. Furthermore, it also assumes another arc to form immediately adjacent to the first one without including any distance of separation between two simultaneously burning arcs. These considerations will result in higher current densities; hence, the large difference in the theoretically and experimentally obtained critical current densities is not surprising. However, the values of the critical current density predicted by the present theoretical model are of the same order as that obtained by Refs. 15 and 16.

The variations of the theoretically predicted critical arc current and critical cathode drop with electrode temperature has been shown in Fig. 7. The critical cathode drop for the transition to big-arcs have been compared with the experimental data obtained in Ref. 19. Furthermore, the experimental data[19] for the current per arc in the micro-arc mode has been reproduced in Fig. 8, which shows the peak value of each arc current pulse and the respective generation frequencies of these arcs. It is seen from this figure that the current per micro-arc remains almost unaffected by the increase in the applied voltage, until the big-arcs, carrying currents of about 100 A or more, appear at a cathode voltage drop of about

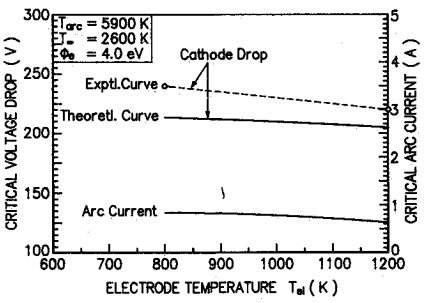

Fig. 7 Dependence of the critical arc current and the critical cathode voltage drop on electrode temperature.

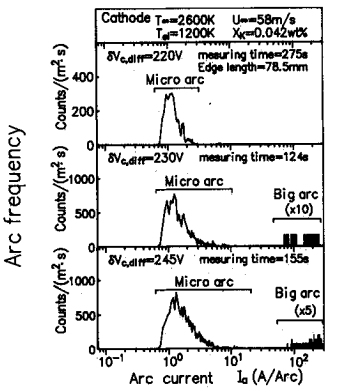

Fig. 8 Frequency spectra of arc pulses with respect to arc current.

230V (T_{el} = 1200 K). No arc pulses were observed between the micro-arc and big-arc stages. It can be seen further that the mean micro-arc current also remained almost constant at about 1.2 A. The value of the critical arc current (about 0.8 A) obtained from the present theoretical analysis (see Fig. 7) is very close to that of the mean micro-arc current (about 1.2 A) obtained in the experiments. The theoretically obtained critical arc current is almost insensitive to electrode temperature variations, indicating only a very slight decrease with increasing electrode temperature. This behavior is exactly identical to that observed in the experiments, where the mean micro-arc current was unaffected by any electrode temperature variations. This implies that the arc transition from micro-arc to big-arc should occur for a critical arc current of above 1 A, irrespective of the electrode parameters.

In the case of the critical cathode voltage drop, as can be seen from Fig. 7, both the theoretical and experimental curves show fairly good agreement. Because the experimental values of the voltage drop are closer to the theoretical predictions for a work function value of 4eV, the calculations have been made throughout for this ϕ_e value. (The high value of ϕ_e should be due to the very low seeding, which causes a low seed coverage on the electrode surface.) As mentioned before, the effect of electrode temperature variations on the critical cathode drop is only slight, with the voltage drop showing a small decrease for an increase in the electrode temperature. This insensitivity is probably associated with the attainment of an almost constant value of the effective work function at the transition stages to the big-arc mode, irrespective of the electrode temperature value. A further increase in electrode temperature should cause a decrease in the arc intensity; hence, in the arc spot temperature, which will also lead to a decrease in the thermionic emission current density (because ϕ_e is constant). This decrease in thermionic emission current density causes the total arc spot current density to decrease; hence, the previously attainable current densities are no longer possible in the micro-arc mode. This makes the arc discharge transition to the big-arc mode occur at lower values of the cathode drop and the plasma current density. This explains the small decrease in the critical values of current density and the cathode drop with increasing electrode temperature.

Figure 9 shows the effect of electrode temperature variations on the critical arc spot and arc column radii. As in the case of the critical arc current, a change in electrode temperature does not have any pronounced effects on the critical arc radii; both the spot radius and the column radius decreasing only slightly with an increase in the electrode temperature. These figures show that the arc transition from micro-arc to big arc and their growth up to or beyond the thermal boundary layer occurs above certain critical arc parameters, which are almost constant, irrespective of the electrode conditions. Furthermore, the good agreement between the theoretical and the experimental values (as seen in Figs. 7 and 8, and also in comparison with results obtained in Refs. 15, 16, and 19) suggests that the basic assumption that the arc transition occurs when the arc height equals the thermal boundary-layer thickness in a reasonable one.

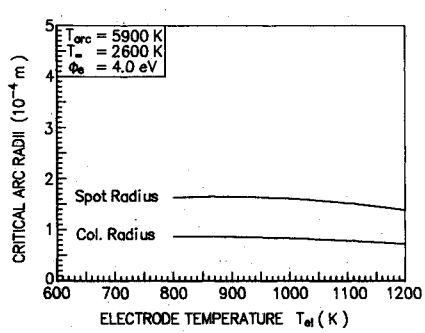

Fig. 9 Variation of the critical arc spot and arc column radii with electrode temperature.

Conclusions

1. The theoretical analysis has been able to predict the critical values for the growth of micro-arcs into big arcs, extending up to or beyond the thermal boundary layers in MHD generator channels, and the cause for such a transition has been clarified.

2. For given plasma conditions, the critical arc parameters for the transition from micro-arcs to big arcs are almost constant.

3. A comparison with experimental data gives a good agreement for critical cathode voltage drops. It also predicts the arc column temperatures during the transition stages to be about 5800–5900 K, under the given experimental conditions.

4. The critical arc current for the transition to big arcs (~1 A) was almost constant, and compared well with the experimentally obtained value for mean micro-arc current (~1.2 A).

5. The comparison of experimental and theoretical voltage drops also predicts the values for the effective work function of the composite cathode surface. It was also found that the arc spot region makes a significant contribution to the overall voltage drop in the micro-arc stages. Furthermore, it is predicted that the surface effects, especially the effective work function of the cathode surface, plays an important role in the micro-arc and the transition stages to the big arcs, but become ineffective after the transition.

References

[1]Messerle, H. K., Sakuntala, M., and Trung, D., "Arc Transition in MHD Generator," *Journal of Physics D: Applied Physics,* Vol. 3, 1970, pp. 1080–88.

[2]Oliver, D. A., "A Constricted Discharge in Magnetohydrodynamic Plasma," *Proceedings of the Fifteenth Symposium on Engineering Aspects of Magnetohydrodynamics,* Paper IX.4, Philadelphia, PA, 1976.

[3]Hsu, M. S. S.; "Thermal Instabilities and Arcs in MHD Boundary Layers," *Proceedings of the Thirteenth Symposium on Engineering Aspects of Magnetohydrodynamics,* Paper VI.6, Stanford, CA, 1973.

[4]Okazaki, K., Mori, Y., Hijikata, K., and Ohtake, K., "Electrothermal Instability in the Seeded Combustion Gas Boundary Layer near Cold Electrodes," *AIAA Journal,* Vol. 16, No. 4, 1978, pp. 334–339.

[5]Okazaki, K., Mori, Y., Hijikata, K., and Ohtake, K., "MHD Boundary Layer of the Seeded Combustion Gas near Cold Electrodes," *AIAA Journal,* Vol. 18, No. 1, 1980, pp. 39–46.

[6]Satheesh, K. A., and Gupta, B., "Electrode Breakdown in Magnetohydrodynamic Plasmas: Stability Analysis," *Journal of Applied Physics,* Vol. 66, 1989, pp. 1610–1617.

[7]Satheesh, K. A., Gupta, B., Tewari, D. P., and Sodha, M. S., "Current Transition in Cathode Boundary Layers of Coal-fired MHD Generators," *Journal of Physics D: Applied Physics,* Vol. 23, 1990, pp. 509–516.

[8]Zalkind, V. I., "The Microarc Operating Regime of MHD Generator Electrodes," *Pridladnaya Matematika i Mekhanika [Journal of Applied Mechanics and Technical Physics],* Vol. 11, No. 1, 1970, pp. 131–135.

[9]Mori, Y., Ohtake, K., and Ogasawara, K., "Heat Transfer of Combustion Gas Plasma in Electric Fields," *Proceedings of the Twelfth Symposium on Engineering Aspects of Magnetohydrodynamics,* Paper II.8, Argonne, IL, 1972.

[10]Koester, J. K., Eustis, R. H., and Rodgers, M. E., "In-Channel Observations on Coal Slag," *Proceedings of the Fifteenth Symposium on Engineering Aspects of Magnetohydrodynamics,* Paper I.6, Philadelphia, PA, 1976.

[11]Zelikson, Y. M., Kirillov, V. V., Reshetov, E. P., and Flid, B. D., "Laws Governing the Operation of Metallic Electrodes of a MHD Generator," *Teplofizika Vysokikh Temperatur [High Temperature],* Vol. 8, Paper 181, 1970.

[12]Harmon-Weiss, E., Unkel, W., Chang, A. Y., and Schwoerer, J., "Anode Phenomena in MHD Generators," *Proceedings of the Twentieth Symposium on Engineering Aspects of Magnetohydrodynamics,* Paper 5.2, Irvine, CA, 1982.

[13]Zalkind, V. I., Kirillov, V. V., Markina, A. P., Tikhotskii, A.

S., and Uspenskaya, G. L., "Experimental Investigation of Cathode Spots on Metallic Electrodes Protruding in Plasma Flow," *Pridladnaya Matematica i Mekhanika [Journal of Applied Mechanics and Technical Physics]*, Vol. 15, 1974, pp. 159–164.

[14]Okazaki, K., Yabe, M., and Okumura, Y., "Separation of Discharge Modes and Transition Behavior of Micro Arc to Big Arc," *Proceedings of the Tenth International Conference on MHD Electrical Power Generation*, Vol. 1, Paper IV.55, Tiruchirapalli, India, 1989.

[15]Buznikov, A. E., Kamalov, Z. G., and Kovbasyuk, V. I., "Contracted Discharge at the Cathode in an MHD Generator," *Teplofizika Vysokikh Temperatur [High Temperature]*, Vol. 25, No. 4, 1988, pp. 470–476.

[16]Buznikov, A. E., Kamalov, Z. G., and Kovbasyuk, V. I., "Constricted Discharge at the Electrodes of Supersonic MHD Generator," *Proceedings of the Tenth International Conference on MHD Electrical Power Generation*, Vol. 2, Paper X.140, Tiruchirapalli, India, 1989.

[17]Satheesh, K. A., and Okazaki, K., "Electrode Surface Effects on the Transition from Micro-arcs to Big-arcs in MHD Generator Channels," *Proceedings of the Meeting of Institute of Electrical Engineers, Japan*, Vol. 2, Paper 13, Sept. 1990, Tokyo, Japan. Also, Satheesh, K. A., and Okazaki, K., communicated to *Journal of Physics D: Applied Physics*.

[18]Rosa, R. J., "Boundary Layer Arc Behavior," *Proceedings of the Eighth International Conference on MHD Electrical Power Generation*, Vol. 1, Paper 251, Moscow, 1983.

[19]Okazaki, K., Okumura, Y., and Yabe, M., "Separation of Discharge Mode and Statistical Characteristics of Arc Generation in the Combustion Gas Plasma Boundary Layer," *Trans. JSME, Ser. B*, Vol. 58, No. 546, 1992, pp. 272–279, (in Japanese).

[20]Nichols, L. D., and Mantenieks, M. A., "Analytical and Experimental Studies of MHD Generator Cathodes Emitting in a Spot Mode," NASA TN D-5414, Sept. 1969.

[21]Rohsenow, W. M., and Choi, H., *Heat, Mass, and Momentum Transfer*, Prentice-Hall, Englewood Cliffs, NJ, 1961, pp. 36–40.

[22]Simola, J., "Erosion Mechanisms and Erosion Rates on Cold Metal MHDG Electrodes," *Proceedings of the Eighth International Conference on MHD Electrical Power Generation*, Vol. IV, Paper 55, Moscow, 1983.

[23]Berkovskii, B. M., Brodskii, A. M., and Tikhotskii, A. S., "Volt-Ampere Characteristic of an Arc Burning at the Electrodes of a Magnetohydrodynamic Generator," *Teplofizika Vysokikh Temperatur [High Temperature]*, Vol. 25, No. 3, 1987, pp. 452–459.

[24]Mitchner, M., and Kruger, C. H., "Partially Ionized Gases," Wiley, New York, 1973, pp. 54–100.

[25]Beilis, I. I., "Arc Discharge and Cathode Erosion of Metallic Electrodes in an MHD Generator Channel," *Proceedings of the Seventh International Conference on MHD Electrical Power Generation*, Vol. 2, Paper 761, Cambridge, MA, 1980.